

37
9/26/90

J.L.R. (2)

IS-M 639

IS-M--639

DE90 018044

NUCLEAR MAGNETIC RESONANCE SURVEY OF HYDROGEN MOTION
AND ELECTRONIC STRUCTURE IN α -PHASE (Nb-Mo)-H ALLOYS

Rodrigo Ibanez-Meier,[#] D. R. Torgeson and R. G. Barnes

Ames Laboratory, USDOE, and Department of Physics,

Iowa State University, Ames, Iowa 50011 USA

ABSTRACT

The results of a proton nuclear magnetic resonance (NMR) survey of hydrogen motion and electronic structure in the solid solution (α) phase of niobium rich $\text{Nb}_{1-y}\text{Mo}_y\text{H}_x$ alloys are reported ($y \leq 0.2$, $x \leq 0.2$). Measurements of the temperature dependence of the proton spin-lattice relaxation time T_1 over the range $20 \leq T \leq 800$ K were analyzed to yield values of the activation energy E_a and jump attempt frequency v_0 for hydrogen diffusive hopping and of the product $T_{1e}T = C_e$ indicative of the electronic density-of-states at the Fermi level, $N(E_F)$, where T_{1e} is that contribution to T_1 . The T_1 vs T behavior shows features characteristic of hydrogen in random alloys, reflecting a distribution of E_a and v_0 values. At high temperatures (~ 500 K), T_1 exhibits anomalous behavior, passing through a maximum and decreasing again at higher temperatures in the same manner found in the Nb-H and (Nb-V)-H systems.

INTRODUCTION

The Mo-H system exhibits many properties that differ from those of the Nb-H system. Mo is not a hydride forming metal, and in contrast to Nb it absorbs hydrogen only endothermally. In addition, the solubility of hydrogen in Mo is extremely low. The metals Nb and Mo have the same

MASTER

DISCLAIMER

This report was prepared as an account of work sponsored by an agency of the United States Government. Neither the United States Government nor any agency thereof, nor any of their employees, makes any warranty, express or implied, or assumes any legal liability or responsibility for the accuracy, completeness, or usefulness of any information, apparatus, product, or process disclosed, or represents that its use would not infringe privately owned rights. Reference herein to any specific commercial product, process, or service by trade name, trademark, manufacturer, or otherwise does not necessarily constitute or imply its endorsement, recommendation, or favoring by the United States Government or any agency thereof. The views and opinions of authors expressed herein do not necessarily state or reflect those of the United States Government or any agency thereof.

DISCLAIMER

Portions of this document may be illegible in electronic image products. Images are produced from the best available original document.

crystal structure (body-centered-cubic), and their atomic radii are very similar ($r_{Nb} = 0.143$ nm, $r_{Mo} = 0.136$ nm), so that when alloyed, they form a continuous series of solid solutions. As Mo is added to Nb, the Nb lattice contracts.

With increasing Mo concentration, the terminal solubility for hydrogen (TSH) in the α phase increases,¹ and the critical transition temperature for the $\alpha-\alpha'$ phase transition is lowered.² The increase in terminal solubility is not due to trapping since the hydrogen solubility in the alloy decreases with increasing Mo content.¹ Recently, Fenzl and Peisl,³ on the basis of theories originally conceived for spin-glasses, showed that hydrogen in alloys can be treated as a lattice gas with random internal fields and random bonds. Their model was applied by Shirley, et al.,⁴ to the Nb-Mo-H system and showed good agreement with the phase diagrams of Fenzl² and Matsumoto, et al.⁵

The present NMR investigation was initiated to compare hydrogen behavior in the Nb-Mo-H system with that in the recently studied Nb-V-H system^{6,7} in which the hydride forming metals Nb and V are also mutually soluble at all concentrations, and in which the TSH increases dramatically. The NMR measurements on that system^{6,7} showed clearly that, in contrast to Nb-H, some hydrogen remained in the solid solution (α) phase down to the lowest temperature at which measurements were made, ~8K. Moreover, in $Nb_{0.5}V_{0.5}H_{0.2}$ no evidence of hydride phase formation was found even at 8K.

EXPERIMENTAL DETAILS

The Nb-Mo alloys were prepared from the highest purity Ames Laboratory metals available. Spark source mass spectroscopy showed the total level of paramagnetic impurities to be less than 10 parts-per-

million (ppm). Hydriding was accomplished in a standard high pressure - high vacuum system evacuated to 2×10^{-7} Torr before heating the electropolished alloy in a Pt boat. Mischmetal trihydride served as the source of high-purity hydrogen. The alloy was heated to 500°C in vacuum and then exposed to a known volume of hydrogen gas for reaction, allowing 12 hours to reach equilibrium. Hydrogen concentrations were initially determined from the hydrogen gas volume and the weight gain of the samples. Final compositions were based on high-temperature vacuum extraction of the hydrogen from portions of the samples. The samples were crushed to a fine powder (< 200 mesh) in a helium-filled glovebox, and sealed in quartz tubes for the NMR measurements.

Proton relaxation rate measurements were made with a phase-coherent pulsed NMR spectrometer that has been described in detail previously.⁸ All of the measurements were made at a resonance frequency of 40 MHz, using the magnetization inversion-recovery pulse sequence. Variable temperature instrumentation for the range 20 - 800 K has also been described.⁷ Standard least-squares data fitting techniques were employed to derive NMR parameter values for both solid solution and hydride phase signals when these were simultaneously present in the magnetization recovery signal.⁷

RESULTS AND DISCUSSION

The α -phase proton spin-lattice relaxation time T_1 was determined for samples with Mo concentrations $y = [\text{Mo}]/[\text{Nb+Mo}] = 0.05, 0.10$ and 0.20 , and hydrogen concentrations $[\text{H}]/[\text{Nb+Mo}] = 0.05, 0.10$ and 0.20 . The samples with higher hydrogen concentrations produced stronger free-induction decay (FID) signals, and hence the α -phase T_1 was easier to follow over a wide temperature range. The samples with lower Mo content

showed non-exponential magnetization recoveries at lower temperatures, indicating the presence of hydride phase precipitates.

We show in Figs. 1(a) and (b) examples of the α -phase T_1 temperature dependence. Fig. 1(a) shows the T_1 behavior over the full temperature range 20-800 K for $\text{Nb}_{0.9}\text{Mo}_{0.1}\text{H}_{0.2}$. Fig. 1(b) shows T_1 behavior over the restricted range 140 - 800 K for the same sample. In this case, the solid curve is a least-squares fit based on a single activation energy for hydrogen diffusive hopping (see further below). The anomalous turn-down of T_1 at high temperatures, which has also been observed in the Nb-H and Nb-V-H systems, for example,⁹ is evident in both figures. As is also evident in Fig. 1(a), the α -phase proton signal continues to be detectable down to the limit of these measurements (~20 K). The same comment applies to the $y = 0.2$, $x = 0.2$ samples.

Nonlinear least-squares fits to the T_1 vs T data were made using the sum of the theoretical expressions for the dipolar relaxation rate, R_{1d} , due to unlike spins (^{93}Nb) and the conduction electron contribution, $R_{1e} = (T_{1e})^{-1} = T/C_e$, where $C_e = T_{1e}T$ is the Korringa product. In these alloys the $^1\text{H} - ^1\text{H}$ dipolar interaction contribution is negligible. Thus, the measured relaxation rate R_1 is

$$R_1 = R_{1d} + R_{1e} \quad (1)$$

with

$$R_{1d} = (1/2) \gamma_I^2 M_2^{\text{IS}} \left[\frac{\tau_c}{1 + (\omega_I - \omega_S)^2 \tau_c^2} + \frac{3\tau_c}{1 + \omega_I^2 \tau_c^2} + \frac{6\tau_c}{1 + (\omega_I - \omega_S)^2 \tau_c^2} \right] \quad (2)$$

where ω_I and ω_S are the 1H and ^{93}Nb Larmor frequencies, respectively, and the correlation time τ_c is taken to be the mean dwell time for hydrogen motion, τ_d , for which Arrhenius behavior is assumed:

$$\tau_d = \tau_0 \exp(E_a/k_B T), \quad (3)$$

with E_a and $\tau_0^{-1} = v_0$ the activation energy and attempt frequency, respectively. M_2^{IS} is the resonance second moment, given by

$$M_2^{IS} = (4/15)C(\gamma_S \hbar)^2 S(S+1) \sum_i (r_i)^{-6} \quad (4)$$

where the sum extends over all metal lattice sites from a generic hydrogen site, with γ_I and γ_S being the 1H and ^{93}Nb gyromagnetic ratios, respectively, S the ^{93}Nb spin and \hbar Planck's constant. For the b.c.c. lattice, with lattice parameter a , and taking hydrogen in a T site, direct computer calculation (based on 8000 metal neighbors), yields for this sum

$$\sum_i (r_i)^{-6} = 146.518 a^{-6} . \quad (5)$$

The factor $C = [Nb]/([Nb]+[Mo])$ takes into account that some sites are occupied by Mo nuclei. ^{95}Mo and ^{97}Mo have very small nuclear moments and low abundances (combined total = 25%), so the only effect of the Mo is to reduce M_2^{IS} by C .

Single Activation Energy

Attempts to fit the T_1 data over the full temperature range using only a single activation energy were unsuccessful. However, the data around the T_1 minimum and on the high temperature side of the minimum could be fit quite well in this way. The solid curve in Fig. 1(b) shows such a fit for the $y = 0.1$, $x = 0.2$ sample. In this procedure, the fit parameters were E_a , τ_0 , M_2^{IS} , and C_e . The results for three sample compositions for which complete data sets were obtained are listed in Table I. In all cases, E_a is approximately the same as that obtained

for Nb-V-H alloys, i.e., 140 meV. This shows that for $T > 180$ K hydrogen motion is essentially controlled by a single activation energy.

Distribution of Activation Energies

Assuming that the motion of hydrogen atoms in a substitutional alloy or structurally disordered (amorphous) solid is governed by a (normalized) distribution of activation energies, $G(E_a)$, the expression for the spin lattice relaxation rate R_{1d} becomes ⁶

$$R_{1d} = \int dE_a G(E_a) R_{1d}(E_a) \quad (6)$$

where $R_{1d}(E_a)$ is given by Eq. (2). In fitting this model to the T_1 data, an asymmetric Gaussian distribution was required, i.e.,

$$G(E_a) = N \exp[-(E_a - E_0)^2/2\sigma^2] \quad (7)$$

where N is a normalizing constant, E_0 is the mid-point energy of the distribution (i.e., the energy at which the two half-Gaussians are joined), and

$$\sigma = \sigma_1 \text{ if } E_a < E_0, \text{ or } \sigma = \sigma_2 \text{ if } E_a \geq E_0.$$

Now in addition to E_0 , τ_0 , M_{2IS} and C_e , the fitting parameters also include the distribution halfwidths σ_1 and σ_2 . The fit obtained in this way to the T_1 data for the $y=0.2$, $x=0.2$ sample is shown by the solid curve in Fig. 2(a), and the distribution function $G(E_a)$ resulting from the fit is shown in Fig. 2(b). Data for the $y = 0.1$, $x = 0.1$ sample could not be fit over the full temperature range with a single distribution, $G(E_a)$. Separate fits were made at high and low temperatures, with C_e determined from the low temperature data, and with E_a and τ_0 determined from the high temperature data.

A significant difference between the present results and those obtained earlier for $Nb_{1-y}V_yH_x$ alloys ⁶ is that a symmetric Gaussian distribution of E_a was obtained in the latter case for $y = 0.25$, $x =$

0.23, for example, in contrast to the present results [Fig. 2(b)]. On the other hand, in the Nb-V-H study, data for $y = 0.1$, $x = 0.1^q$ could also not be fit over the full temperature range with a single distribution of E_a values.⁶ Indeed, the results of the Nb-V-H study suggest that a transition occurs from long-range diffusive hopping motion at high temperatures to "localized" motion in the neighborhood of the V atoms at low temperatures, concurrent with precipitation of the hydride phase.

The values of the Korringa products C_e are similar to those obtained in Nb-V-H alloys.⁶ However, several factors contribute to the difficulty of deriving reliable C_e values. First, motional relaxation (R_{1d}) is still very strong at low temperatures. Second, an additional complication results from proton spin cross-relaxation to the ^{93}Nb spins.¹⁰ This mechanism is especially effective at low temperatures and low resonance frequencies, adding another rate process R_{1cr} with the result that the measured rate is $R_{1e} + R_{1cr}$. Neglect of R_{1cr} in the present case could result in the analysis yielding anomalously small C_e values. For comparison, in the case of $\text{Nb}_{0.5}\text{V}_{0.5}\text{H}_{0.23}$ the value $C_e = 110 \text{ s K}$ was obtained at a measuring frequency of 40 MHz,⁶ whereas $C_e = 59 \text{ s K}$ was obtained at 127.5 MHz which is well above the frequency range of cross-relaxation interactions.¹⁰ This shows that C_e can be a sensitive function of measuring frequency.

The second moment values M_2^{IS} obtained from fitting the data using either model are substantially smaller than the calculated value based on Eq's. (4) and (5), i.e., 29.5 (0e)^2 . There are two causes for this. Since nearest-neighbor Nb atoms contribute most strongly to M_2^{IS} , those hydrogen atoms that occupy sites having an Mo nearest neighbor experi-

ence a smaller M_2^{IS} . In addition, due to the distribution of E_a values, the interaction strength, i.e., $\gamma_1^2 M_2^{IS} \tau_0$, is distributed over the entire low temperature range of T_1 values rather than concentrated at the T_1 minimum.

ACKNOWLEDGMENTS

The authors are indebted to B. J. Beaudry and N. Beymer for their careful preparation of the samples for the NMR measurements. Ames Laboratory is operated for the U. S. Department of Energy by Iowa State University under Contract No. W-7405-Eng-82. This work was supported by the Director for Energy Research, Office of Basic Energy Sciences.

REFERENCES

- # Present address: Department of Physics, Rice University, Houston, TX 77251.
- 1. A. Inoune, M. Katsura and T. Sano, J. Less-Common Met. 55, 9 (1977).
- 2. W. Fenzl, Ph.D. Dissertation, Universitat Munchen, 1983 unpublished.
- 3. W. Fenzl and J. Peisl, Phys. Rev. Letters 54, 2064 (1985).
- 4. A. I. Shirley, C. K. Hall, P. S. Sahni and N. J. P. King, J. Chem. Phys. 81, 4053 (1984).
- 5. T. Matsumoto, Y. Sasaki and M. Hirara, J. Phys. Chem. Solids 36, 215 (1974).
- 6. L. R. Lichty, J. Shinar, R. G. Barnes, D. R. Torgeson and D. T. Peterson, Phys. Rev. Lett. 55, 2895 (1985).
- 7. L. R. Lichty, Ph. D. Dissertation, Iowa State University, 1988 unpublished.

8. T-T. Phua, B. J. Beaudry, D. T. Peterson, D. R. Torgeson, R. G. Barnes, M. Belhoul, G. A. Styles and E. F. W. Seymour, Phys. Rev. B 26, 6227 (1983).
9. J-W. Han, L. R. Lichty, D. R. Torgeson, E. F. W. Seymour, R. G. Barnes, J. L. Billeter and R. M. Cotts, Phys. Rev. B 40, 9025 (1990)
10. L. R. Lichty, J-W. Han, D. R. Torgeson, R. G. Barnes and E. F. W. Seymour, Phys. Rev. B (in press).

FIGURE CAPTIONS

Fig. 1. Temperature dependence of the proton T_1 in $\text{Nb}_{0.9}\text{Mo}_{0.1}\text{H}_{0.2}$ over (a) the full temperature range 25 - 800 K and (b) over the restricted range 140 - 800 K. The solid curve in (b) is the least-squares fit of Eq's. (1) and (2) in the text using a single activation energy, excluding the two lowest temperature data points shown in the figure.

Fig. 2. (a) Temperature dependence of the proton T_1 in $\text{Nb}_{0.8}\text{Mo}_{0.2}\text{H}_{0.2}$ over the full temperature range 20 - 800 K. The solid curve is the least-squares fit of Eq's. (1) and (2) in the text using a distribution of activation energies. (b) The distribution of activation energies that results from fitting the T_1 data shown in (a).

Table I. Parameters determined by least-squares fit of Eq's. (1) and (2) to the high temperature proton T_1 data using a single activation energy, E_a . The τ_0 values are estimated to be uncertain by a factor of 2.

Composition	τ_0 (10^{-12} s)	E_a (meV)	M_2^{IS} (0e) 2	C_e (s K)
$Nb_{0.9}Mo_{0.1}H_{0.1}$	2	140 ± 15	9.9	140 ± 40
$Nb_{0.9}Mo_{0.1}H_{0.2}$	2	145 ± 15	9.4	152 ± 45
$Nb_{0.8}Mo_{0.2}H_{0.2}$	2	130 ± 15	11.8	250 ± 70

Table II. Parameters determined by least-squares fit of Eq's. (1) and (2) to the full temperature range of proton T_1 data using a distribution of activation energies, $G(E_a)$. The τ_0 values are estimated to be uncertain by a factor of 2.

Composition	τ_0 (10^{-12} s)	E_0 (meV)	σ_1 (meV)	σ_2 (meV)	M_2^{IS} (0e) 2	C_e (s K)
$Nb_{0.8}Mo_{0.2}H_{0.2}$	2	210 ± 20	55	3	25.6	120 ± 15
Low temperature						
$Nb_{0.9}Mo_{0.1}H_{0.1}$	2	140 ± 15	35	30	10.3	170 ± 20
High temperature						
$Nb_{0.9}Mo_{0.1}H_{0.1}$	2	140 ± 15	4	4	10.3	170 ± 20

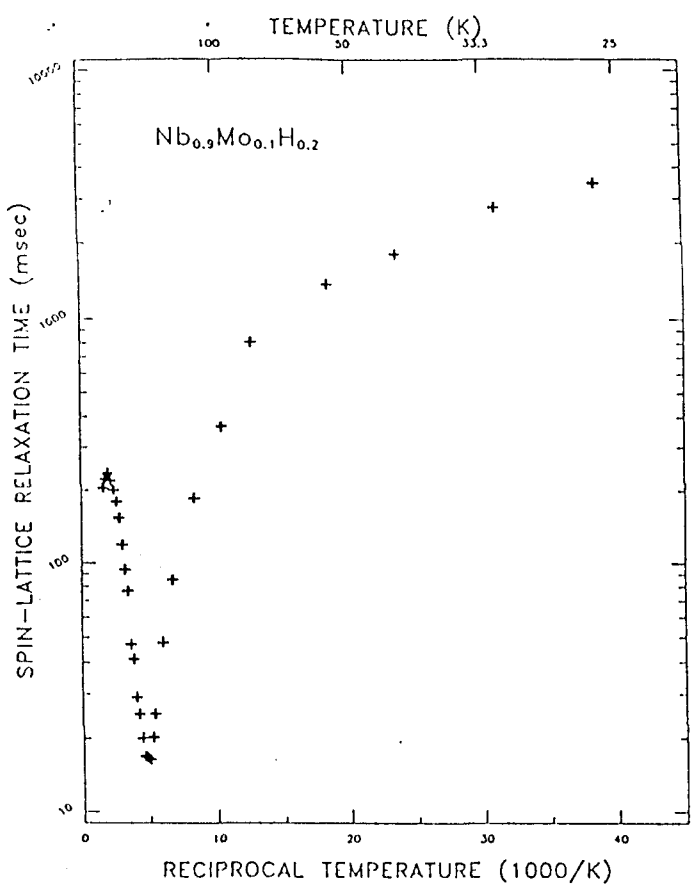


Figure 1(a)

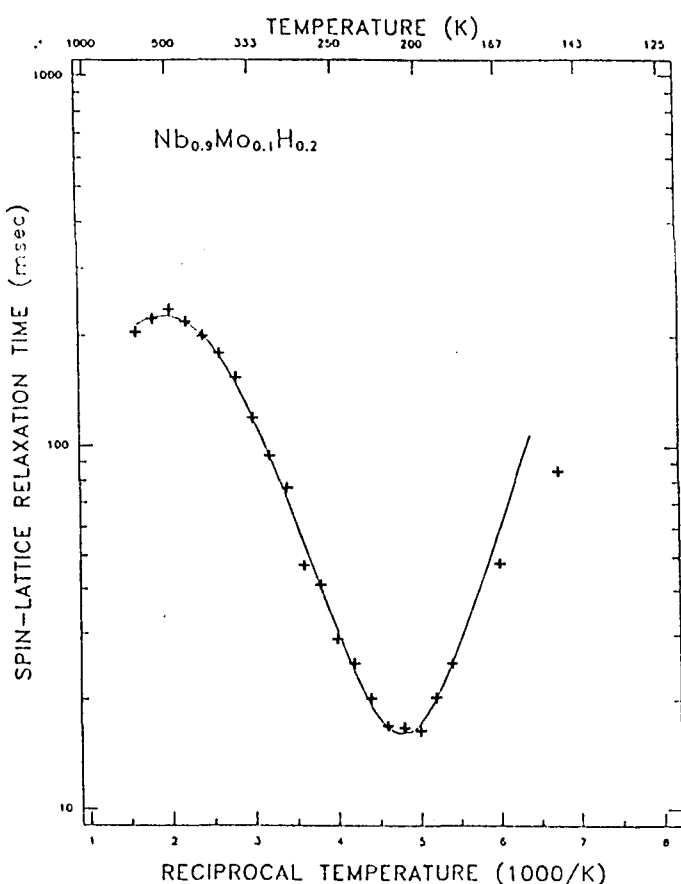


Figure 1(b)

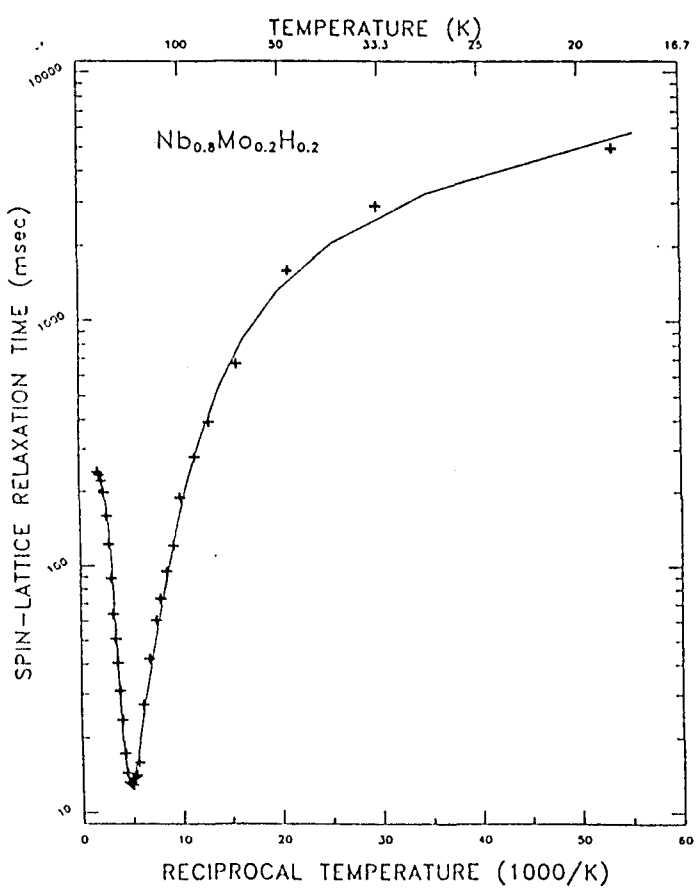


Figure 2(a)

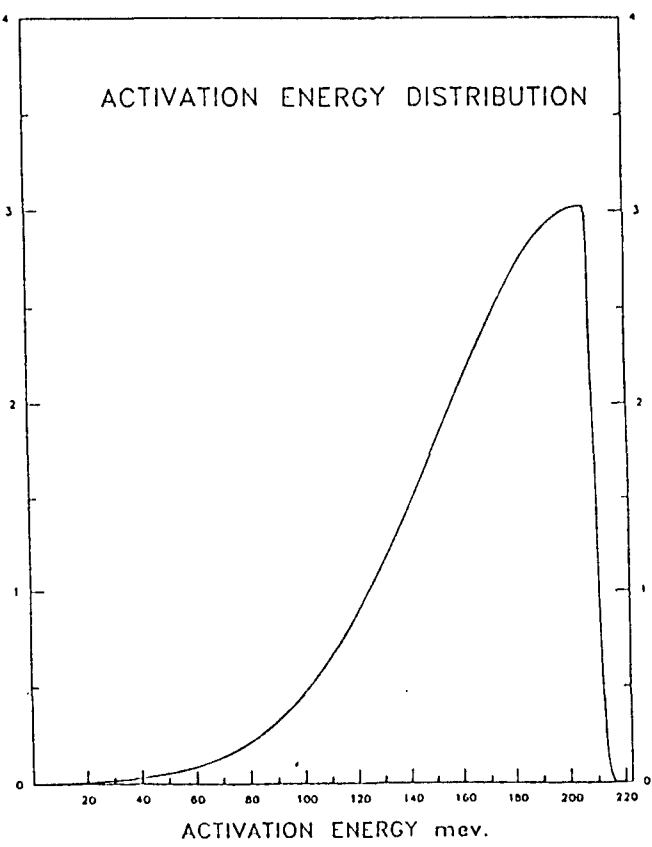


Figure 2(b)